

RSC Advances



This is an *Accepted Manuscript*, which has been through the Royal Society of Chemistry peer review process and has been accepted for publication.

Accepted Manuscripts are published online shortly after acceptance, before technical editing, formatting and proof reading. Using this free service, authors can make their results available to the community, in citable form, before we publish the edited article. This *Accepted Manuscript* will be replaced by the edited, formatted and paginated article as soon as this is available.

You can find more information about *Accepted Manuscripts* in the [Information for Authors](#).

Please note that technical editing may introduce minor changes to the text and/or graphics, which may alter content. The journal's standard [Terms & Conditions](#) and the [Ethical guidelines](#) still apply. In no event shall the Royal Society of Chemistry be held responsible for any errors or omissions in this *Accepted Manuscript* or any consequences arising from the use of any information it contains.

Fabrication of paper micro-devices with wax jetting

Zong'an Li^{1,*}, Jiquan Yang², Li Zhu³ and Wencheng Tang¹

¹ Southeast University, Nanjing, Jiangsu, CHINA 1; 101000185@seu.edu.cn

² Nanjing Normal University, Nanjing, Jiangsu, CHINA 2; 63047@nynu.edu.cn

³ Nanjing University of Science and Technology, Nanjing, Jiangsu, CHINA; zhuli@njjust.edu.cn

* Correspondence: zonganli@seu.edu.cn; Tel.: +86-136-751-07447

Abstract: Paper microfluidic devices are a promising technology in developing analytical devices for point-of-care diagnosis in developing world. This article described a novel method of wax jetting with a PZT (Piezoelectric Ceramic Transducer) actuator and glass nozzle for the fabrication of paper microfluidic devices. The hydrophobic fluid pattern was formed by the permeation of filter paper with wax droplets. Result showed that the size of the wax droplet which was determined by the voltage of the driving signal and nozzle diameter ranged from 150 μ m to 380 μ m, and coefficient of variation of the droplet diameter was under 4.0%. The smallest width of the fluid channel was 600 μ m of frontside and 750 μ m of backside. The patterned filter paper was without any leakage, and multi-assay of glucose, protein, and PH on paper microfluidic device, and laminar diffusion flow with blue and yellow dye were realized. The wax jetting system supplied a low-cost, simple, easy-to-use and fast fabrication method for paper microfluidic device.

Keywords: paper microfluidic devices; wax jetting; bio-assay, micro mixing.

1. Introduction

The paper microfluidics device is a very important kind of platform for point-of-care diagnostics and environment monitoring. It uses small volumes of sample and paper is made of naturally abundant materials and biodegradable. Many researchers have put lots of effort on the paper based micro fluidic as it has advantages of easy to use, inexpensive, low volume, easily adaptable, and are capable of rapid on-site detection [1-3].

To realize low cost and simple paper microfluidic devices, many kinds of fabrication methods have been developed, such as photolithography[4-6], plotting **Error! Reference source not found.**, inkjet etching[8-12], plasma etching[13], flexographic printing[14-16], cutting[17-21], stamp [22-23] and wax printing[24-25]. In conditions of micro reaction or analysis, the hydrophobic patterns of on the paper need to be changed frequently or to be very complicate, and this requires that the fabrication methods are low cost and fast. The photolithography [4-6], plasma etching [13], flexographic printing [14-16], water resist ink plotting [7] and stamp or punch method [22-23] need metal or other kinds of templates. The processing of templates requires multi steps and not easily adaptable. Paper devices by knife, punch or laser cutting [17-21] are not easy to be folded and stored. The wax printing method was very promising as the wax material is easily available and biodegradable. The commercial wax 3D (three-dimensional) printer and its suited wax were expensive. The need still remains for gentle and simple fabrication techniques of paper microfluidic devices that can be widely implemented in developing world at minimized cost.

In this paper, the paper microfluidic device was fabricated with a novel method of wax jetting which was based on PZT actuator and a home-made glass nozzle. The jetted wax droplets were linked with each other and melted into the paper to form into hydrophobic

barriers. Firstly, the relationship between the size of the wax droplets and the system parameter was determined. The wax droplets were linked with each other on the glass slide using 3D printing table. Then, the relation between the wax barrier and printing width and the resolution of the wax jetting method on filter were experimentally studied. Finally the paper device were fabricated and tested. Multi bio-assays of glucose, protein, and PH, and stable micro diffusion of blue dye and yellow dye were presented.

2. Materials and method

2.1. Materials

Qualitative filter paper 102 \varnothing 7 cm and \varnothing 10cm were from Hangzhou Xinhua Paper Industry Co., Ltd. Glass nozzle 1.0mm \times 0.6 mm was from Nanjing Lupu Chemical Co., Ltd. Paraffin wax 56-58 was supplied by Shanghai Specimen and Model Factory. Glucose oxidase (Amresco 0243), horseradish peroxidase(JS10540, Cas 9003-99-0, RZ \geq 1.5), Bovine serum albumin (BSA), tetrabromophenol blue (TBPB) (MW 691.9), glucose, erioglucine disodium salt (BR, 85%, 3844-45-9) and tartrazine BS (85% 1934-21-0) were purchased from Shanghai Jinsui Bio-tec Co., Ltd. Potassium iodide, ethanol AR Citrate and trisodium citrate dehydrate were from Nanjing Chemical Reagent Co., Ltd.

2.2. Wax droplet generating system

A wax droplet generator on a 3D printing work table was used to prepare the paper microfluidic devices. The wax droplet generator consist of a piezoelectric actuator (Polytec PI P-844.10), a glass nozzle, a wax container and a connector as shown in the figure 1. The photograph of the droplet generating system was shown in the figure S1. The glass nozzle was made out of a borosilicate glass tube with inside diameter of 0.6 mm and outside of 1.0 mm. The glass tube was first pulled with a micropipette puller (Sutter P2000/G) and then cut with a ceramic chip on the tip leaving an outlet diameter of 150 μ m. After that, the glass nozzle was forged with a micronozzle processor of Narishige MF-900 leaving the final outlet diameter ranged from 50 μ m to 100 μ m as shown in the figure S2. The glass nozzle was bonded to an aluminum connector which was screwed on a wax container made of aluminum. The temperature was controlled by a heating rod and a thermocouple probe.

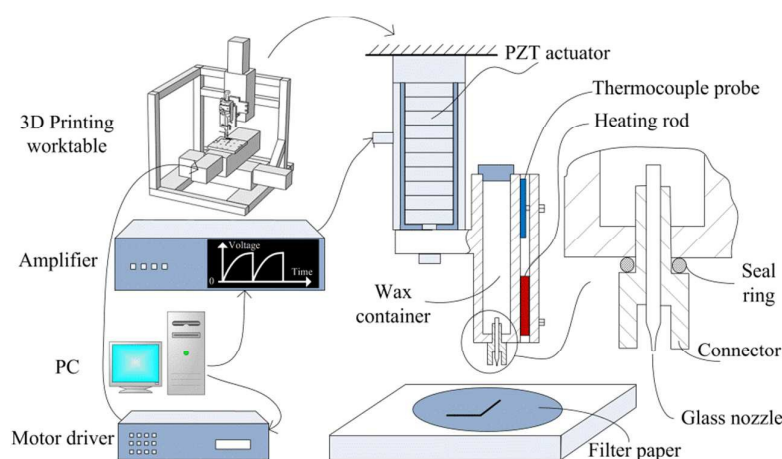


Figure 1. Schematic of the wax droplet generating system

The drop-on-demand wax droplet generating was proposed on the inertia force of the fluid body as shown in the figure 2. The signal received by the PZT actuator was shown in the figure 1. The stack PZT was charged gently and discharged sharply. Because of the

piezoelectric effect, the glass nozzle gets a speed v in the constricting direction by the force F as shown in the figure 2. There exists a thin fluid boundary layer near the glass wall and the fluid outside this layer gets a relative speed v_1 cause by inertia. The jetting happened under the action of viscous force F_1 and inertia force F_2 .

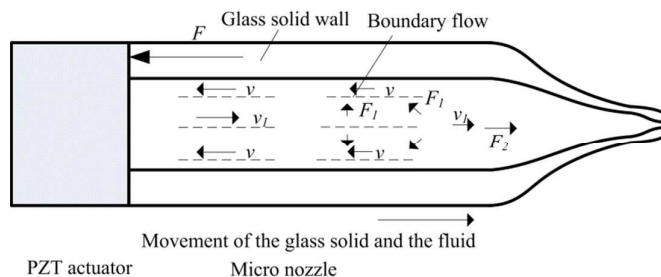


Figure 2. Principle of microfluidic driving

2.3. Jetting of wax droplet

The cylinder wax container with length of 45 mm and diameter of 7 mm was filled with paraffin wax and covered to avoid dust in the air. The wax was melted and injected to the container with a syringe and a syringe filter (filter mesh: 0.45 μm). The jetting temperature is 95 $^{\circ}\text{C}$. This is an improvement compared with the glass nozzle [26] as there is no need to control the maximum length of the wax liquid in the nozzle to avoid extruding and the fabrication process was easy to control. By the peak voltage of the driving signal ranged from 30 V to 80 V, the wax was jetted on the glass slide with 50 μm , 75 μm and 100 μm glass nozzle.

2.4. Bio-assay using paper microfluidic devices

The paper microfluidic devices were tested with 2000 mM erioglucine (blue dye) and 1870 mM tartrazine (yellow dye) solution. 30 μL of blue dye and 30 μL of yellow dye were slowly dipped in the feeding area of the paper devices respectively. The BSA assay were realized by dipping 3 μL of a 250 mM citrate buffer solution (pH 1.8) in the reaction zone and followed by 3 μL of 3.3 mM TBPB solution in 95% ethanol. The glucose assay were realized by dipping 3 μL of potassium iodide solution and followed by 3 μL of 1:5 horseradish peroxidase/glucose oxidase solution (100 unites/mL). For the PH detection, 3 μL of PH reagent were dipped in the reaction zone.

Devices with eight circular reaction zones were used for different concentration solution assay. For BSA assay, 3 μL of BSA solution of 0, 1, 4, 10, 25, 66, 90, 130 mg/mL were dipped in A–H zones separately. Devices with four circular reaction zones was used for multi-assay, 30 μL of a mixture of 50 mM of glucose solution and 7.5 mM of BSA solution with 1:1 ratio was dipped in the middle of the cross area.

3. Result and discussion

3.1. Preparation of wax droplets

The SEM (Scanning Electron Microscope) photo of 5 \times 7 wax droplet array jetted by a micro nozzle with 75 μm outlet diameter, 45 V peak voltage and 3 Hz signal was shown in the figure 3. The diameter of droplet outline circle was 218 μm . The coefficient of variation (CV) of the diameter of the jetted wax droplets was under 4.0% which showed a well uniformity. In a range of 1 Hz -15 Hz, the signal frequency had little influence on the wax droplet size. The

relationship between the wax droplet diameter and the peak voltage of the driving signal and outlet diameter of the glass nozzle was shown in the figure 4.

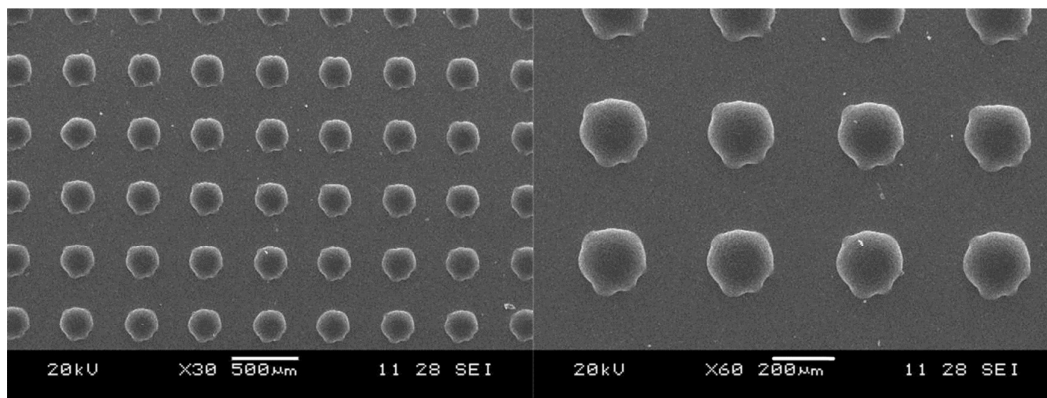


Figure 3. SEM photo of wax droplet array formed on the glass slide

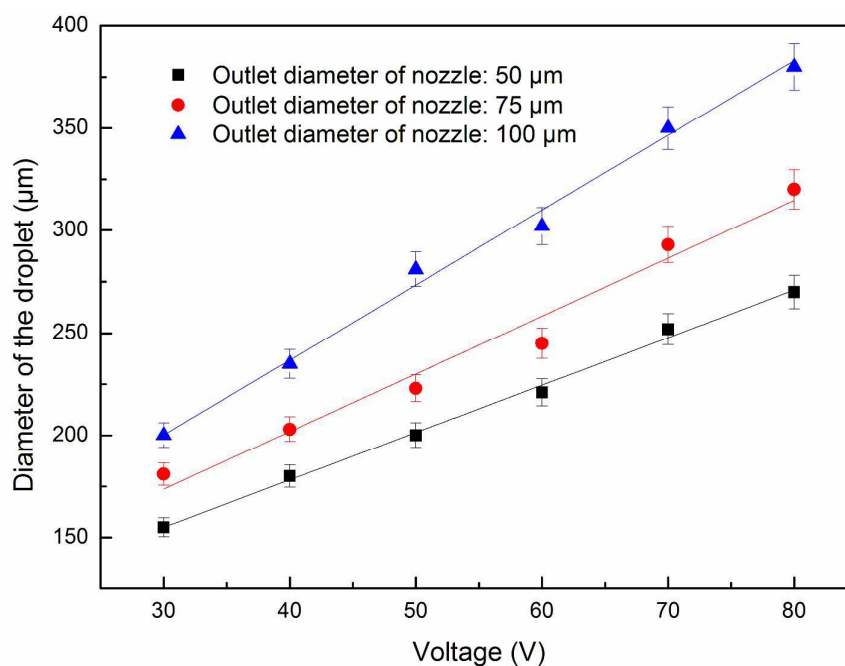


Figure 4. Relationship between wax droplet diameter and the peak voltage of the driving signal and outlet diameter of the glass nozzle

3.2. Preparation of wax line on glass slide

The barrier “wall” in the filter paper was formed by the wax material melted into the paper, and the wax line was prepared by linking of wax droplets with each other. We defined the degree of overlapping (k) to represent the amount of wax material per unit length as shown in the figure 5 and k could be written as (1), where L was the length of the overlap area (μm); D was the outline circle diameter of a wax droplet (μm); v was the moving speed of the 3D printing worktable ($\mu\text{m/s}$); f was the jetting frequency. The choosing of k was determined by the thickness of the filter paper and the size of the wax droplet. When the overlapping was less than 0, none of the wax droplets linked with each other, and k was more than 80%, wax droplets grew from the glass slide into an inclined pillar.

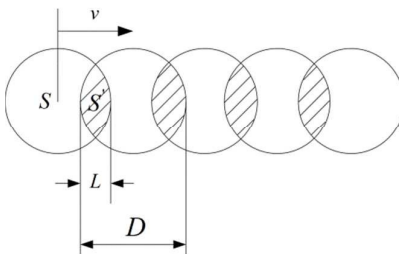


Figure 5. Schematic diagram of the wax droplets

By adjusting the moving speed of the 3D printing worktable (v), k could be changed. Thus, v could be written as $v = D(f - 1)(1 - k)$. For our system, v was less than 50 mm/s and the resolution was 1 $\mu\text{m/s}$. With the micro nozzle of 75 μm outlet diameter, 40 V peak voltage and 11 Hz signal, wax lines with k under 0 and $k = 10\%$, 30%, 50% and 70% were prepared respectively. Results were shown in the figure 6. When the wax droplets did not link, they were round with diameter of 200 μm . Once k was more than 0, a wax tail formed in the moving direction and grew into the neighbor wax droplet and they link with each other to form into line shape. The top surface of wax line with $k=50\%$ was smoother than that of $k=10\%$, and the number of the wax droplets could be read from the bottom surface relief. When $k=70\%$, the width of the wax line was nonuniform and the wax wall grew higher than that of $k=50\%$.

$$k = \frac{L}{D} = 1 - \frac{v}{(f - 1)D} \quad (1)$$

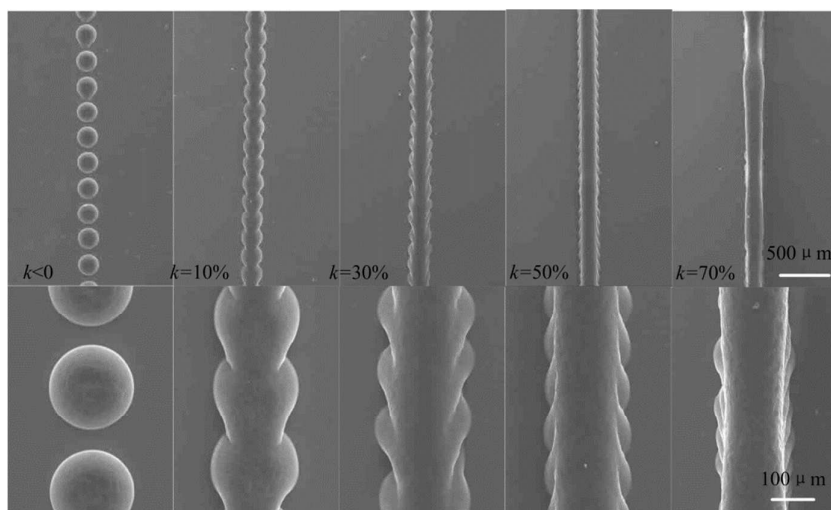


Figure 6. SEM photo of wax line on glass slide (a) Wax droplets unlinked with each other (b) Wax line prepared with $k=10\%$, (c) $k=30\%$, (d) $k=50\%$ (e) $k=70\%$

3.3. Relation between the wax barrier and printing width

Traditional paper diagnostic that used for the glucose, protein or urine is strip like which could only test one kind of element in the agent. Patterned paper combining multi channel and reaction zones enabled multi assay with capillary flow. Our previous work has proved that $k=50\%$ and kept in 75 $\circ\text{C}$ thermostatic well for 80 seconds is fine for the penetration of the filter paper with thickness of 90 μm [26].

The relation between the final front wax barrier width and printing width was studied. Outlet diameters of glass nozzles were 50 μm , 75 μm and 100 μm , and degree of overlapping

(k) was 50%. To make the wax to penetrate the filter paper sufficiently and save time, the filter paper was kept on a heating plate of $120\text{ }^{\circ}\text{C}$ for 10 seconds. The printing width was determined by the diameter of wax droplets. The wax barriers with width of $950\text{ }\mu\text{m}$, $1050\text{ }\mu\text{m}$ and $1200\text{ }\mu\text{m}$ are shown in the figure 7. As the transparency of filter paper could be improved by the penetration of wax, the color depth increased with the barrier width. The relation between the wax barrier and printing width is shown in the figure 8, and the wax barrier width ranged from $770\text{ }\mu\text{m}$ to $1200\text{ }\mu\text{m}$.

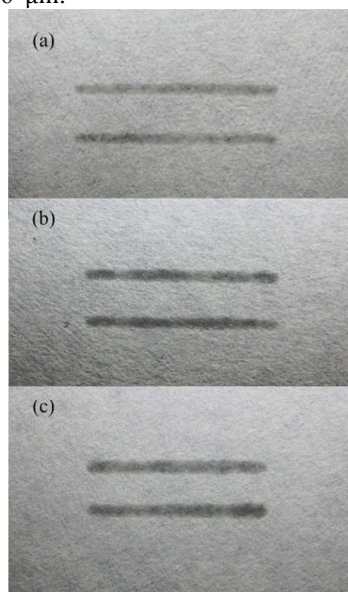


Figure 7. Wax barriers on filter paper with thickness of $90\text{ }\mu\text{m}$, (a) Wax barriers with width of $950\text{ }\mu\text{m}$, (b) Wax barriers with width of $950\text{ }\mu\text{m}$, (c) Wax barriers with width of $1200\text{ }\mu\text{m}$

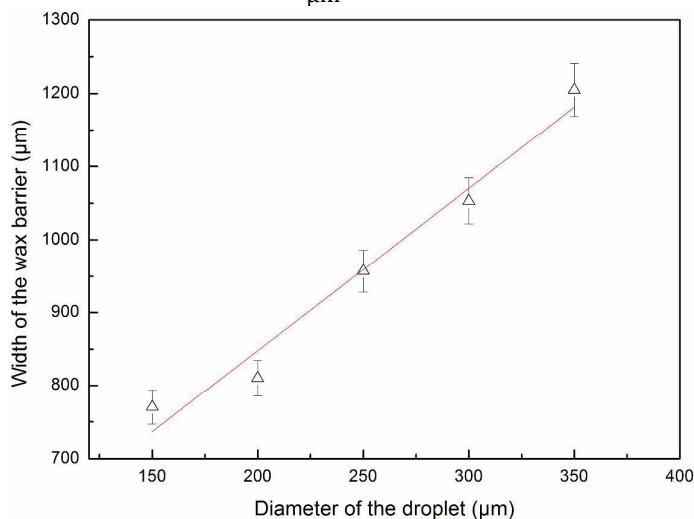


Figure 8. Relation between the wax barrier and printing width

3.4. Resolution of wax jetting on filter paper

The resolution of the wax jetting method on filter paper was presented by the final width of fluid channels. With the barrier width of $770\text{ }\mu\text{m}$, leakage may happen along the fluid channel. The jetting conditions are as follows: outlet diameter of the micro nozzle is $75\text{ }\mu\text{m}$ forged from $150\text{ }\mu\text{m}$, the peak voltage of the driving signal is 40 V , the frequency is 11 Hz and the moving speed of the worktable is 1 mm/s ($k=50\%$). The fluid pattern is made up of 8

reservoirs with 10 mm channel sharing the same feeding pool. The designed channel width on AutoCAD increases from 800 μm to 2200 μm in 200 μm steps. Result showed that the 800 μm and 1000 μm fluid channels designed were totally blocked and the yellow dye flow into part of the 1200 μm fluid channel. The reservoirs with designed channel width of 1400 μm and more were totally wetted by capillary flow. The front and back side of the paper device are shown in the figure 9 and S3.

The smallest channel width allowing solution to wet the entire reservoir through 10 mm channel was found to be 600 μm in front side and 750 μm in back as shown in the figure 10. The resolution of wax jetting method is limited by the thickness, porosity, and orientation of paper fibers as well as the smallest wax droplet size jetted on the paper. Moreover, we studied the width consistency along 10 mm channel from 1400 μm to 2200 μm in 200 μm steps. The channel width was measured 15 times with step of 600 μm along the back side, and 10 times with step of 900 μm for the frontside channel. Result showed that the relative standard deviation was less than 11.0% for all front and back channel widths as shown in the table S1 and S2.

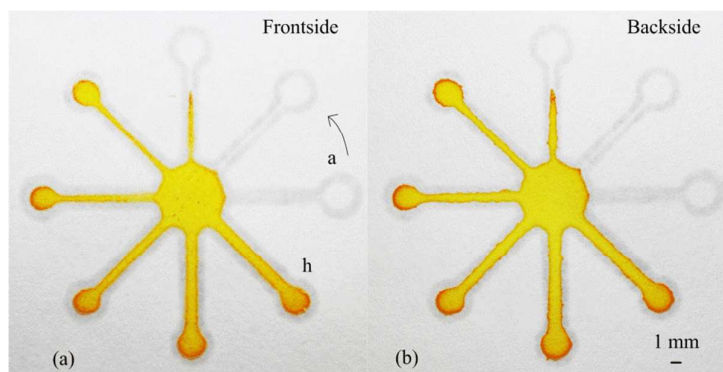


Figure 9. The paper microfluidic devices with designed fluid channel widths from a-800 μm to h-2200 μm in 200 μm steps on AutoCAD, (a) Front side of the paper device filled with yellow dye solution, (a) Back side of the paper device

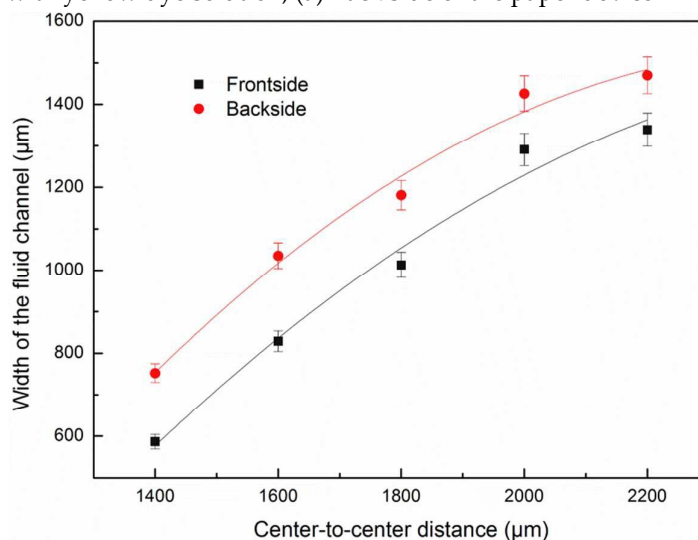


Figure 10. The channel width of front side and backside formed by wax barriers with center-to-center distance from from 1400 μm to 2200 μm in 200 μm steps

3.5. Test of paper device used for multi-assay

The paraffin wax was jetted on the filter paper to form the pattern designed for bio-assay. Wax patterns for multi-assay with eight circular reaction zones, eight square reaction zones

and five polygon zones were prepared respectively. With capillarity of filter paper, the solution reached the reaction zones for multi-assay in 3 minutes without any leakage. The wax patterns dried after 15 minutes are shown in the figure 11.

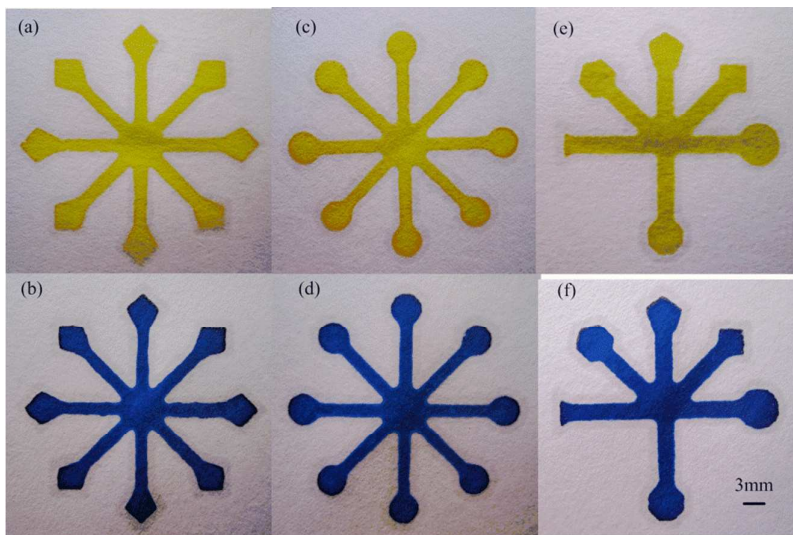


Figure 11. (a, b) Paper microfluidic devices with eight square reaction zones for multi-assay filled with yellow dye and blue dye (c, d) Devices with eight circular reaction zones filled with yellow dye and blue dye (e, f) Devices with five polygon reaction zones filled with yellow dye and blue dye

3.6. Multi-assay using paper micro devices

Results of the multi-assay were shown in the figure 12. After 10 minutes of dipping the BSA solution to zones A to H respectively, the color of reaction zones from A to H changed from aquamarine blue to cobalt blue as the concentration increased as shown in the figure 12 (a). For the multi-assay, after 5 minutes of dipping the sample solution, zone A appeared a yellow coffee ring showing the presentation of glucose and inlet area of zone B turned blue as the existence of BSA. Zone C turned light yellow in the whole area indicating that the PH was 7.0 as shown in the figure 12 (b).

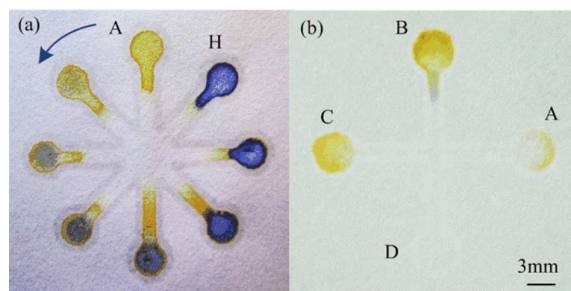


Figure 12. (a) Protein assay, 10 minutes after respectively dipping $3\mu\text{L}$ of 0, 1, 4, 10, 25, 66, 90, 130 mg/mL of BSA solution on zone A-H, (b) Multi-assay for $30\mu\text{L}$ mixture of 25 mM glucose and 3.75 mM of BSA solution, 5 minutes after dipping of the test agent.

3.7. Lamiar flow diffusion using paper micro devices

Traditional transverse diffusion across adjacent flow stream is usually realized with Y shape micro channels with two or more inlet to study inter diffusion of one or multiple species, to evaluate transport processes, and to sense analytes ranging from pH to

immunoassay targets [27]. The capillary flow in paper was extremely stable which enabled a very stable diffusion interface and thus need not extremely stable pumps. Micro mixers with two-dimensional paper networks were designed with two and three inlet areas. The diffusion area was laid with a source pad made from lens paper to keep the dye solution.

The wax pattern of paper device with two inlet area is shown in the figure 9-a. Assuming the inlet area is an infinite source and the absorbent area is an infinite sink, the flow in a fully wetted paper device is approximated by Darcy's law:

$$Q = -\frac{\kappa wh}{\mu L} \Delta P \quad (2)$$

Where Q is volumetric flow rate, κ is the permeability of the paper, wh is the area of the channel cross-section with width, w , and height, h , μ is the dynamic viscosity, and ΔP is the pressure drop occurring over the length, L , of the paper channel.

For the designed filter paper microfluidic device in the figure 9-b, κ and μ are constant. For the inlet channels, $w_1 = w_2$ and $L_1 = L_2$. When the same amount of sample solutions are dipped in the left and right source area, $\Delta P_1 = \Delta P_2$. Deduced from $Q_1 = Q_3$ and $Q_2 = Q_4$, we could get $w_3 = w_4$. The diffusion coefficient γ was defined by ratio of width of the diffusion area and the flow channel in the outlet area. γ is written as:

$$\gamma = \frac{2L_3 \tan \frac{\theta}{2}}{w_3 + w_4} \quad (3)$$

For the device with two inlets, 100 μL of yellow dye was dipped in the inlet zone A, and 100 μL of blue dye into the inlet zone B in the same time. The laminar flow of blue branch and yellow branch had a clear boundary in the beginning. The blue and yellow dye diffused into each other along with the fluid channel and the interface turned green as shown in the figure 13. Calculated by device dipped of solutions after 10 minutes, the diffusion coefficient γ was 46.9%.

For the device three inlets, 100 μL of yellow dye was dipped in the inlet zone A and C, and 100 μL of blue dye into the inlet zone B in the same time. The yellow and blue dye met in the reaction channel and divided into three branches with yellow, blue and green colors. The interface between the yellow and blue branches turned green by diffusion, and the area of green color increased along with the capillary flow as shown in the figure 14. Calculated by device dipped of solutions after 10 minutes, the diffusion coefficient γ as defined before was 57.1%.

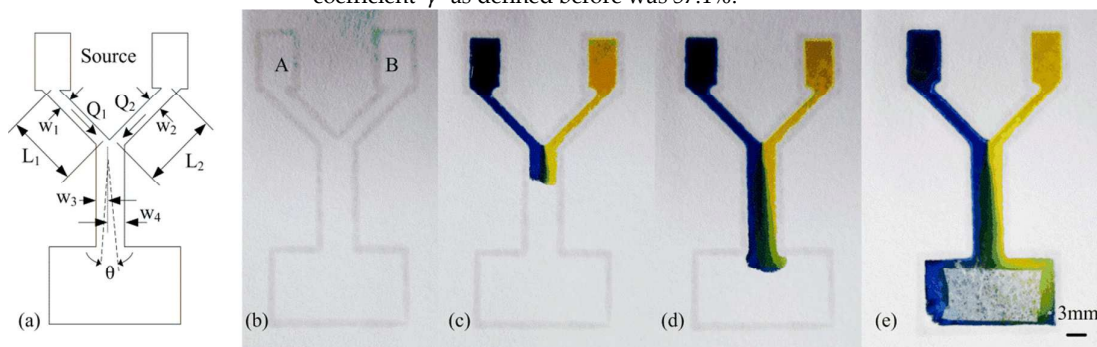


Figure 13. Micro diffusion of blue and yellow dye in the device with two inlet areas (a) Schematic of the paper device, the diffusion coefficient γ was defined by ratio of width of the diffusion area and the flow channel in the outlet area. (b) Before dipping (c) After 40 seconds, (d) After 2 minutes, (e) after 10 minutes

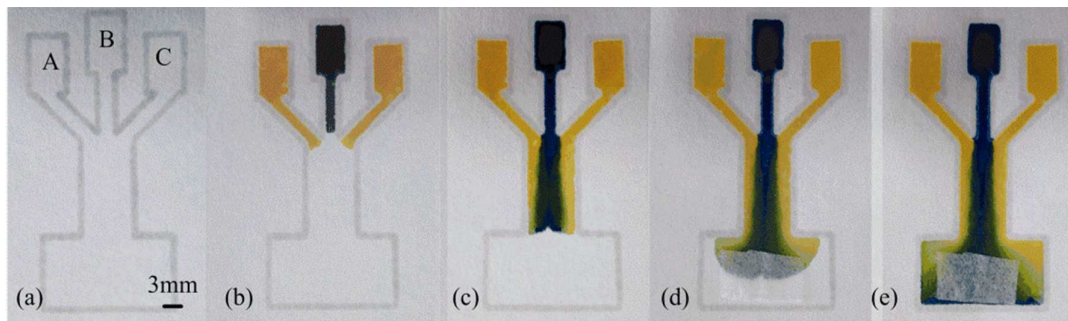


Figure 14. Micro diffusion of blue and yellow dye in the device with three inlet areas (a) Before dipping (b)After 20seconds, (c) After 2 minutes, (d) After 5 minutes, (e) After 10 minutes

4. Conclusions

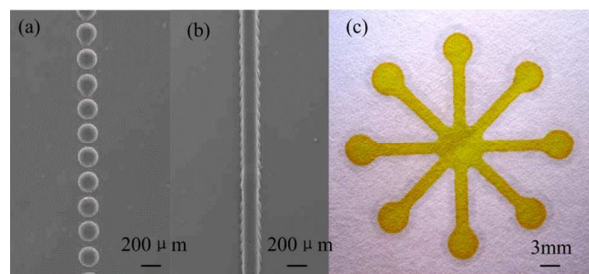
The paper microfluidic devices were fabricated with wax jetting by a PZT stack actuator, glass nozzle and 3D printing worktable. The wax jetting was a promising fast and easy method for the fabrication of paper microfluidic devices for the point of care or other experimental study. The wax material(0.0019 \$/g) and the glass capillary tube (0.0078 \$ per piece) was cheap and easy available. The paper microfluidic devices need not any templates or multiple printing steps, whereas the pattern is formed directly on the paper and only need to be designed on the computer, which saved the time and cost. The patterned filter paper by the wax droplets was without any leakage, and multi-assay of glucose, protein, and PH on paper microfluidic device, and laminar diffusion flow with blue and yellow dye could be realized. This method also supplied a fast and easy way for the scientific researchers to develop new types of paper microfluidics.

Acknowledgments: This paper is supported by the National Natural Science Foundation of China (no. 61273243, no. 51407095), Program of Natural Science Research of Jiangsu Higher Education Institutions of China(Grant No.14KJB480004), Program of Natural Science Foundation of Jiangsu Province (BK20150973) , the Fundamental Research Funds for the Central Universities.

References

1. Yamada, K.; Henares, T. G.; Suzuki, K.; Citterio, D. Paper-Based Inkjet-Printed Microfluidic Analytical Devices. *Angewandte Chemie International Edition*. 2015, 54(18), 5294-5310.
2. He, Y.; Wu, Y.; Fu, J. Z.; Wu, W. B. Fabrication of paper-based microfluidic analysis devices: a review. *RSC Advances*, 2015, 5(95), 78109-78127.
3. Cate, D. M.; Adkins, J. A.; Mettakoonpitak, J.; Henry, C. S. Recent Developments in Paper-Based Microfluidic Devices. *Analytical chemistry*, 2014, 87(1), 19-41.
4. Yu, L.; Shi, Z. Z. Microfluidic paper-based analytical devices fabricated by low-cost photolithography and embossing of Parafilm. *Lab on a Chip*, 2015, 15(7), 1642-1645.
5. San Park, T.; Baynes, C.; Cho, S. I.; Yoon, J. Y. Paper microfluidics for red wine tasting. *RSC Advances*, 2014, 4(46), 24356-24362.
6. Martinez, A. W.; Phillips, S. T.; Wiley, B. J.; Gupta, M.; Whitesides, G. M. FLASH: a rapid method for prototyping paper-based microfluidic devices. *Lab on a Chip*, 2008, 8(12), 2146-2150.
7. Nie, J.; Zhang, Y.; Lin, L.; Zhou, C.; Li, S.; Zhang, L.; Li, J. Low-cost fabrication of paper-based microfluidic devices by one-step plotting. *Analytical chemistry*, 2012, 84(15), 6331-6335. Nie, Z.; Deiss, F.; Liu, X.;
8. Akbulut, O.; Whitesides, G. M. Integration of paper-based microfluidic devices with commercial electrochemical readers. *Lab on a Chip*, 2010, 10(22), 3163-3169.

9. Wang, J.; Monton, M. R. N.; Zhang, X.; Filipe, C. D.; Pelton, R.; Brennan, J. D. Hydrophobic sol-gel channel patterning strategies for paper-based microfluidics. *Lab on a Chip*, 2014, 14(4), 691-695.
10. Elsharkawy, M.; Schutzius, T. M.; Megaridis, C. M. Inkjet patterned super hydrophobic paper for open-air surface microfluidic devices. *Lab on a Chip*, 2014, 14(6), 1168-1175.
11. Yamada, K.; Takaki, S.; Komuro, N.; Suzuki, K.; Citterio, D. An antibody-free microfluidic paper-based analytical device for the determination of tear fluid lactoferrin by fluorescence sensitization of Tb 3+. *Analyst*, 2014, 139(7), 1637-1643.
12. Maejima, K.; Tomikawa, S.; Suzuki, K.; Citterio, D. Inkjet printing: an integrated and green chemical approach to microfluidic paper-based analytical devices. *Rsc Advances*, 2013, 3(24), 9258-9263.
13. Li, X.; Tian, J.; Shen, W. Quantitative biomarker assay with microfluidic paper-based analytical devices. *Analytical and bioanalytical chemistry*, 2010, 396(1), 495-501.
14. Määttänen, A.; Fors, D.; Wang, S.; Valtakari, D.; Ihalainen, P.; Peltonen, J. Paper-based planar reaction arrays for printed diagnostics. *Sensors and Actuators B: Chemical*, 2011, 160(1), 1404-1412.
15. Sameenoi, Y.; Nongkai, P. N.; Nouanthavong, S.; Henry, C. S.; Nacapricha, D. One-step polymer screen-printing for microfluidic paper-based analytical device (μ PAD) fabrication. *Analyst*, 2014, 139(24), 6580-6588.
16. Dungchai, W.; Chailapakul, O.; Henry, C. S. A low-cost, simple, and rapid fabrication method for paper-based microfluidics using wax screen-printing. *Analyst*, 2011, 136(1), 77-82.
17. Fenton, E. M.; Mascarenas, M. R.; López, G. P.; Sibbett, S. S. Multiplex lateral-flow test strips fabricated by two-dimensional shaping. *ACS applied materials & interfaces*, 2009, 1(1), 124-129.
18. Nie, J.; Liang, Y.; Zhang, Y.; Le, S.; Li, D.; Zhang, S. One-step patterning of hollow microstructures in paper by laser cutting to create microfluidic analytical devices. *Analyst*, 2013, 138(2), 671-676.
19. Fang, X.; Wei, S.; Kong, J. Paper-based microfluidics with high resolution, cut on a glass fiber membrane for bioassays. *Lab on a Chip*, 2014, 14(5), 911-915.
20. Mu, X.; Zhang, L.; Chang, S.; Cui, W.; Zheng, Z. Multiplex microfluidic paper-based immunoassay for the diagnosis of hepatitis C virus infection. *Analytical chemistry*, 2014, 86(11), 5338-5344.
21. Sun, M.; Johnson, M. A. Measurement of total antioxidant capacity in sub- μ L blood samples using craft paper-based analytical devices. *RSC Advances*, 2015, 5(69), 55633-55639.
22. Perozzello, G.; Candeloro, P.; Gentile, F.; Nicastrì, A.; Perri, A.; Coluccio, M. L.; Di Fabrizio, E. Microfluidics & nanotechnology: towards fully integrated analytical devices for the detection of cancer biomarkers. *RSC Advances*, 2014, 4(98), 55590-55598.
23. Thuo, M. M.; Martinez, R. V.; Lan, W. J.; Liu, X.; Barber, J.; Atkinson, M. B.; Whitesides, G. M. Fabrication of Low-Cost Paper-Based Microfluidic Devices by Embossing or Cut-and-Stack Methods. *Chemistry of Materials*, 2014, 26(14), 4230-4237.
24. Renault, C.; Koehne, J.; Ricco, A. J.; Crooks, R. M. Three-dimensional wax patterning of paper fluidic devices. *Langmuir*, 2014, 30(23), 7030-7036.
25. Chaiyo, S.; Siangproh, W.; Apilux, A.; Chailapakul, O. Highly selective and sensitive paper-based colorimetric sensor using thiosulfate catalytic etching of silver nanoplates for trace determination of copper ions. *Analytica chimica acta*, 2015, 866, 75-83.
26. Li, Z.; Hou, L.; Zhang, W.; Zhu, L. Preparation of paper micro-fluidic devices used in bio-assay based on drop-on-demand wax droplet generation. *Analytical Methods*, 2014, 6(3), 878-885.
27. Esquivel, J. P.; Del Campo, F. J.; de la Fuente, J. G.; Rojas, S.; Sabate, N. Microfluidic fuel cells on paper: meeting the power needs of next generation lateral flow devices. *Energy Environmental Science*, 2014, 7(5), 1744-1749.



(a) Wax droplets of 200 μm jetted on glass slide (b) Wax line on glass slide with degree of overlapping 50% (c) Paper micro fluidic device running with yellow dye for multi-assay